

Microparticle-assisted 2D super resolution virtual image modeling

Bekirov A.R., Zengbo W., Luk'yanchuk B.S.

ABSTRACT

The approach that makes it possible to explain the phenomenon of super resolution in a virtual image using dielectric microparticles is presented. A resolution of the order of 50 nm in the visible range is demonstrated. The presented two-dimensional model uses the FDTD code to generate radiation and its propagation through a microparticle-object system and the following optical image generation using backward propagation technique.

INTRODUCTION

The wave nature of light limits the size of objects that can be observed using an optical microscope. According to the Abbe criterion, it is impossible to distinguish two point incoherent sources if the distance between them is less than half of the wavelength $\lambda/2$ of the emitted radiation. In [1] it was shown that by examining objects with the help of dielectric microparticles, it is possible to resolve structures beyond the diffraction limit. Various theories have been proposed to explain this phenomenon [2-10]. However, no clear explanation of the nature of this phenomenon has been presented. In order to explain the theoretical problems, it is necessary to consider in more detail way the process of image formation by a microparticle. It is convenient to carry out this consideration using geometric optics.

While observing an object through a microsphere, for example, a point source, the ray path is changed due to refraction at the microparticle boundary, see Fig. 1. As a result, a magnified virtual image is formed. The observed distance between the two sources also increases, however, it would be a mistake to say that such consideration can explain the overcoming of the diffraction limit. The rays forming the virtual image are concentrated inside a cone whose boundaries touch the surface of the sphere. As a result, the numerical aperture that forms the image is limited, and blurring of the image occurs, which compensates for the gain due to magnification. In addition, because of aberration not all refracted rays converge at one point.

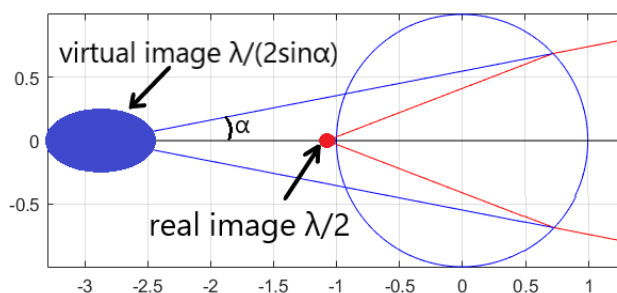


Fig. 1. Geometric path of rays from a point source. Red rays are the actual path of the rays, blue ones form a virtual image and are a continuation of the red ones during reverse propagation. The blue and red dots show the size for the real and virtual images. The image in the virtual case is significantly blurred due to the limited aperture.

This consideration was carried out from the standpoint of geometric optics, which has a limited area; in our example, the condition of applicability is the smallness of the light wavelength compared to the particle size. In experiments, the particle size ranges from several to tens of wavelengths [1, 11]. Thus, it is advisable to consider this problem from the standpoint of wave optics. However, the wave theory in the most of cases demonstrates agreement with geometric

considerations [5]. The exception is resonance cases. In [4], it was firstly demonstrated that when exciting the whispering gallery modes with a dipole, it is possible to increase the resolution to $\lambda/4$. However, as emphasized in the work, this requires a very special choice of the wavelength or a radius of the sphere. Typically, in experiments, super-resolution is observed using a broadband light source in microparticles of various sizes. Thus, a correct theory should not rely on resonance phenomena of this type. In addition, the distributions presented in [4] for the image field have significant “noise” around the focusing point, which is also not observed in the experiment.

The situation changes significantly when the substrate is taken into account. In this case, there are rays arising due to re-reflection of the “sphere-substrate” type. In work [12], we showed that in a particle-on-substrate system it is possible to form magnification without blurring. The resolution of $\lambda/8$ was showed. However, some modification in the solution is required: changing in the source field or changing in the scattering matrix of the sphere. In both cases, the required amendments made a huge contribution to the original solution. It is important to note that such the amendments are the only ones! Thus, despite the fact that the work was of a very formal nature, it showed that the required properties of the system to overcome the diffraction limit differ significantly from those considered before. It suggests that it is necessary to consider more complex effects, such as interaction between the microparticle and the object by means of light scattering. To this end, we propose to consider a complete simulation of the propagation of radiation from an object through a microparticle and the following image formation. Due to the large requirements for computing power, we will limit ourselves to the two-dimensional case.

RESULTS

To present our model we start from simulation of the results from work [1]. The experiment used an incoherent source in the form of a halogen lamp. The first step requires constructing a source field. We used data on the spectrum of this source from work [2], see Fig. 2, since in the original work only the peak wavelength was indicated. Note that further results do not change if we consider a uniform spectrum from 425 nm to 675 nm. To simulate incoherent source field we used point sources with random frequency and initial phase. The wavelengths are distributed with probability according to the spectrum in Fig. 2. The initial phases had a uniform distribution from 0 to 2π .

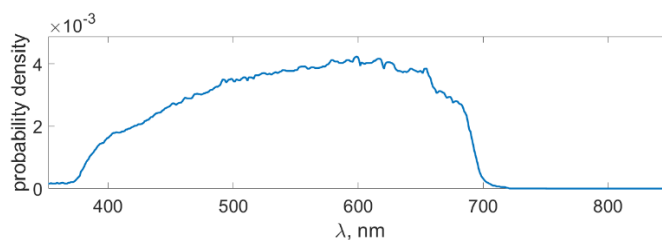


Fig. 2. Probability density distribution for source frequencies used in our the calculations according to the halogen lamp source [2].

In our simulation we used 2D FDTD method in the TE geometry ($E_z=0$) implemented in the Lumerical MODE package. Note that we used a custom time signals in the form of a continuous emission, rather than a single pulse. To construct the image, we used the idea of backpropagation of radiation. For this purpose, the same 2D FDTD method implemented in the custom Matlab code was used. In order to generate an image, the radiation sources must be real fields, but taken in reverse time. In our example, the source can be specified based on a single component H_z :

$$H_z^{image\ source}(x, y = y_0, t) = H_z^{real\ field}(x, y = y_0, -t). \quad (1)$$

To record the real field, we used time-monitors located above the microparticle. Both reflecting and transmitting imaging mode were investigating, the calculation scheme is presented in Fig. 2. For simulation in reflection mode, sources should be placed above the microparticle. In order to exclude the field of sources when the field is reversed in time, we used directed Gaussian sources, implemented in Lumerical. In this case, the source field extends only towards the object. For transmitted mode we used dipole sources placed below the sample. Note that the resulting image field does not depend on the location of reversal plane y_o , provided that the distance to the particle much bigger than λ . In our calculations this distance was about $2.5 \mu m$. To present time-independent result we use time averaging of the image field intensity:

$$I^{image}(x, y) = 1/T \int_0^T |\mathbf{E}^{image}(x, y, t)|^2 dt, \quad (2)$$

here T - is the total simulation time.

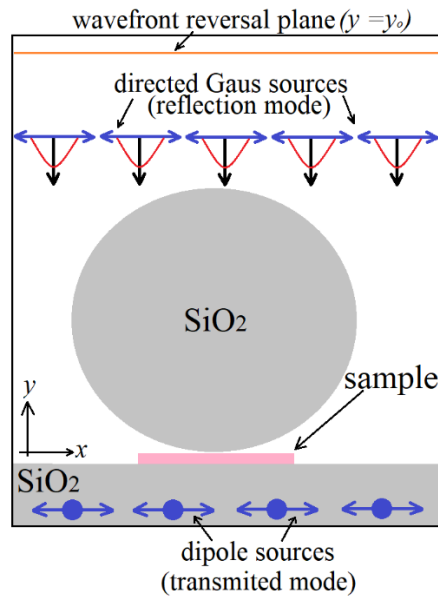


Fig. 2. The calculation scheme.

Firstly, we simulate super resolution for slits in metal screen. In this case, the sample was observed in the transmitted light mode. The sample is a 30 nm thick perfect electric conductive (PEC) screen coated on the glass substrate with four 360 nm wide slits at the distance of 130 nm . The glass microparticle (SiO_2) with a radius of $2.37 \mu m$ is located above the slits according to Fig. 3 c). We simulated four slits offset from the center of the sphere to ensure that the maxima in the image field actually identify the location and number of slits. The sources were located inside the glass substrate $3 \mu m$ below the slits. The simulation time was 1000 fs , repeated 100 times and averaged over all implementations. The simulation results present in Fig. 3. According to the results presented in Fig. 3, the microparticle makes it possible to distinguish slits, while in free space they are indistinguishable. We plotted the square of the average intensity $(I^{image})^2$, which does not affect on the resolution but gives better contrast. The three maxima in Fig. 3 b) arise due to the limited averaging time.

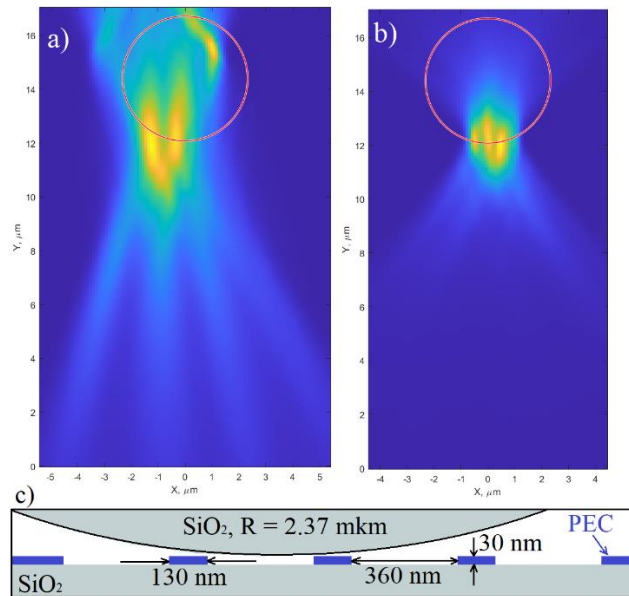


Fig. 3. a, b) – time-averaged image field with and without a microparticle, respectively, red circle is a boundary of the particle. Comparing distributions a) and b) we can conclude that the gaps are indistinguishable without the presence of a microparticle. For better contrast we used square of the values (2) c) general calculation scheme, four 360 nm slits with a step of 130 nm between them in a 30 nm thick perfect conductive screen. The entire system is located on a glass substrate, inside of which there are sources with a random phase and frequency. A glass sphere with a radius of 2.37 μm is located above the slits.

Next, we consider Blue ray DVD disk super resolution in the reflection mode. We presented the DVD disc as perfect conductors embedded in SiO_2 with dimensions corresponding to the DVD disc, 20 nm thickness perfect conductors 200 nm wide at 100 nm distance, see Fig 4 c). In order to show that resonance effects do not play a role in this case we took the radius of the particle $R = 2.35 \mu\text{m}$. The simulation result present in Fig. 4.

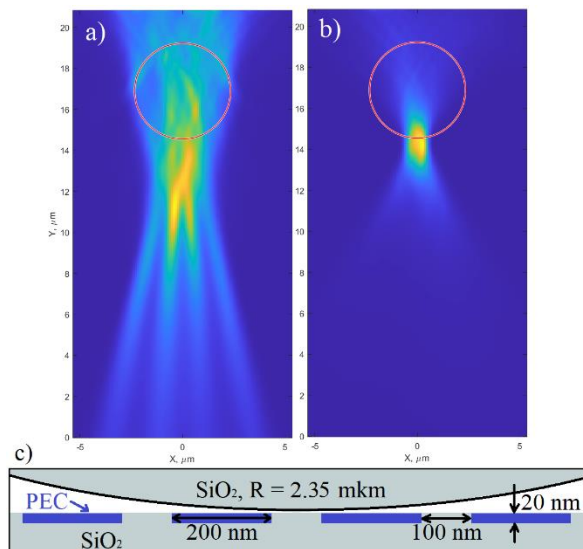


Fig. 4. a, b) – time-averaged image field in reflection mode with and without the microparticle, respectively. Comparing distributions a) and b) we can conclude that the gaps are indistinguishable without the presence of a microparticle. For better contrast we used square of the values (2) c) general calculation scheme, four perfect conductors 200 nm wide at 100 nm distance.

Next, we will look at image simulation for 50 nm pores in gold-coated anodic aluminium oxide (AAO) membrane. Modeling a sample over its entire thickness is a very cumbersome task, so we limited the aluminum layer to 600 nm, the gold layer is 30 nm. The entire sample is divided into 50 nm pores with 50 nm distances between them. The microparticle size is similar to the previous

calculation, $R = 3 \mu\text{m}$. The radiation sources were placed at a distance of 300 nm from the lower boundary of aluminum. The simulation results are presented in Fig. 5.

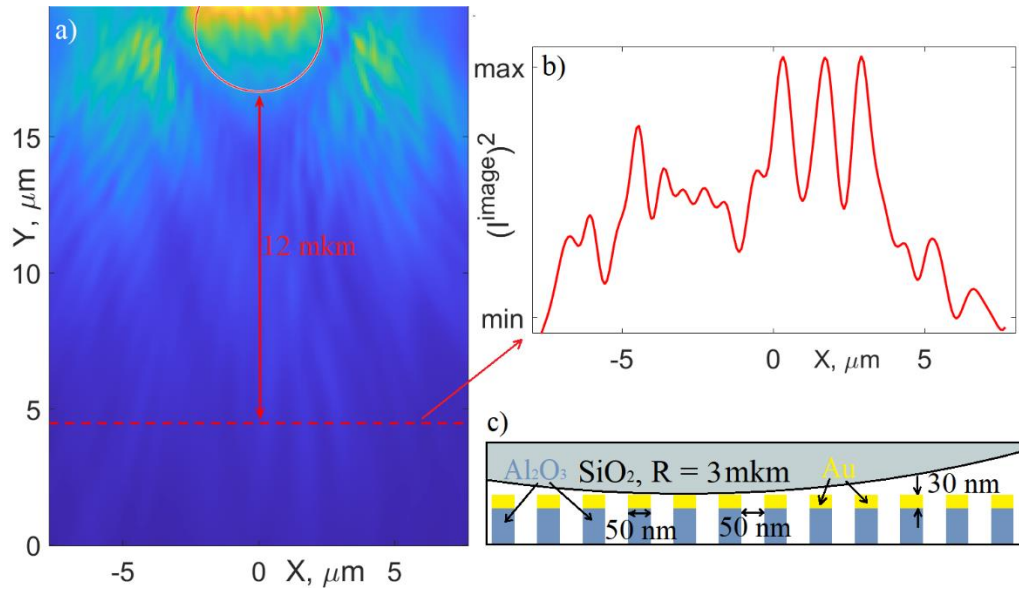


Fig. 5. a) time-averaged image field, red circle is a boundary of the particle, the red line indicates the slice in which three pronounced maxima can be observed. b) image field at a distance of $12 \mu\text{m}$ below the screen. c) sample geometry, 50 nm pores with a distance of 50 nm between them in a $2 \mu\text{m}$ thick aluminum substrate and 30 nm gold.

At a distance of $12 \mu\text{m}$ below the substrate, three pronounced maxima can be observed. However, it would be a mistake to assume that the resolution is 50 nm . Because the two distinct pores remain indistinguishable. Thus, from our simulations, we can conclude that the presented experiment is not reliable evidence of super resolution of 50 nm , since we see only some maxima but cannot claim that these maxima correspond to several adjacent pores.

For a more reliable check, you should consider individual objects rather than periodic ones. For this purpose, we considered a similar calculation, but for only several objects. In works [14-15] individual objects were observed at distances of the order of 50 nm . The imaging was performed by a scanning laser confocal microscope operating at $\lambda = 405 \text{ nm}$. According to that scheme we simulate super resolution for two perfect conductive 120 nm wide dimers at 60 nm distance according to work [14] and three 136 nm wide particles at 25 nm distance according to [15]. We used a reflection mod, similar to what we did for the DVD disc above. All sources had the same wavelength $\lambda = 405 \text{ nm}$, but random initial phase. We used the same material SiO_2 for microparticle. The obtained results presented in Fig. 6. Both cases demonstrate super resolution for fixed wavelength $\lambda = 405 \text{ nm}$ of source as it was observed in experiment. The three particles in Fig. 6 b) are barely distinguishable, which indicates the maximum resolution for this system. We also carried out the calculation in the absence of microparticles. In both cases the picture does not change, the structures are not distinguishable.

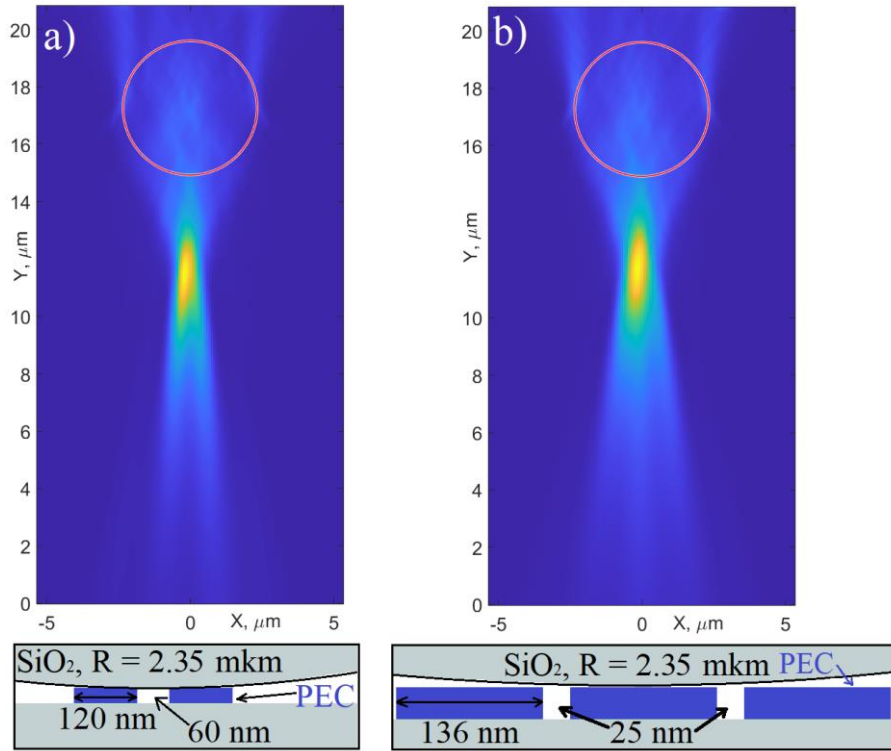


Fig. 6. Virtual image in the reflection mode with $\lambda = 405 \text{ nm}$ for a) 120 nm wide dimers at 60 nm distance, b) three 136 nm wide particles at 25 nm distance. The calculation geometry is showed in the bellow panels. The particles height in both cases is 30 nm. The three particles in b) are barely distinguishable, which indicates the maximum resolution for this system.

The presented calculations state that the source field and its spectrum is a crucial parameter for microparticles assisted super resolution technique. The optical resolution criterion $\lambda/2$ accepted in the literature refers to two point sources. The question of the applicability of this criterion to real objects is widely discussed [8, 15], in particular whether the distance between the edges of structures should be compared or with their centers.

If we consider a particle that is not separated by gaps, we can observe pronounced maxima, which are almost completely similar to the case with the gaps. For the case in Fig. 6 b), in the absence of the gaps, time averaging leads to the fact that these three maxima merge into one, while in the presence of the gaps these maxima remain distinguishable. The situation is different in the case of Fig. 6 a); even in the absence of the gap, two pronounced maxima can be observed, which do not disappear upon averaging. Thus, although the two particles are distinguishable, in our calculations they are indistinguishable from the case of a single particle without the gap. A comparison of these results indicates that the optical resolution may depend on what type of structure we are considering. In all the presented results, the spectrum of the source contains wavelengths comparable to the size of the structures, which allows us to conclude that the sphere increases contrast, not resolution. Another fact indicating an increase in contrast is that two point sources at a distance of 25 nm are indistinguishable.

Our model is still not complete, 2D simulation does not allow to simulate more complex shapes, as a triangle or star. In addition, we used ideal conductors to model the structures, which significantly reduced the overall modeling time. However, the results we presented can serve as a reliable foundation for further 3D modeling. Moreover, when using the FDTD method, we could have missed resonance solutions.

CONCLUSIONS

This paper presents a calculation that makes it possible to explain most of the phenomena observed in [1, 12-13]. Our results provide convincing evidence of the distinguishability of structures with dimensions similar to Blue-ray DVD discs. We have shown that when considering AAO structure with a period of about 50 nm, pronounced maxima can be observed in the virtual image. We cannot attribute their presence to super-resolution at these scales, since we cannot distinguish individual objects at such a distance for halogen lamp source. We showed super resolution of the order of 50 nm at a wavelength of $\lambda = 405$ nm as it was in [14-15]. Our calculations show that microparticle assisted microscopy allows to distinguish objects comparable with wavelength of light even the distance between them much less.

BIBLIOGRAPHY

- [1] Wang, Zengbo, et al. "Optical virtual imaging at 50 nm lateral resolution with a white-light nanoscope." *Nature communications* 2.1 (2011): 218.
- [2] Yang, Hui, et al. "Super-resolution imaging of a dielectric microsphere is governed by the waist of its photonic nanojet." *Nano letters* 16.8 (2016): 4862-4870.
- [3] Boudoukha, Rayenne, et al. "Near-to far-field coupling of evanescent waves by glass microspheres." *Photonics*. Vol. 8. No. 3. MDPI, 2021.
- [4] Duan, Yubo, George Barbastathis, and Baile Zhang. "Classical imaging theory of a microlens with super-resolution." *Optics letters* 38.16 (2013): 2988-2990.
- [5] Bekirov, Arlen Remzievich, B. S. Luk'yanchuk, and Andrei Anatol'evich Fedyanin. "Virtual image within a transparent dielectric sphere." *JETP Letters* 112.6 (2020): 341-345.
- [6] Pahl, Tobias, et al. "FEM-based modeling of microsphere-enhanced interferometry." *Light: Advanced Manufacturing* 3.4 (2022): 699-711.
- [7] Simovski, Constantin, and Reza Heydarian. "A simple glass microsphere may put the end to the metamaterial superlens story." *AIP Conference Proceedings*. Vol. 2300. No. 1. AIP Publishing, 2020.
- [8] Astratov, Vasily N., et al. "Roadmap on Label-Free Super-Resolution Imaging." *Laser & Photonics Reviews* 17.12 (2023): 2200029.
- [9] Maslov, A. V. "Effect of boundary conditions in modeling of microsphere-assisted imaging." *Applied Optics* 63.16 (2024): 4372-4379.
- [10] A. V. Maslov and V. N. Astratov, "Origin of the super-resolution of microsphere-assisted imaging," *Appl. Phys. Lett.* 124 (6), 061105 (2024);
- [11] Lee, Seoungjun, et al. "Overcoming the diffraction limit induced by microsphere optical nanoscopy." *Journal of Optics* 15.12 (2013): 125710.
- [12] Bekirov, A. R. "On superresolution in virtual image in a transparent dielectric sphere." *Optics and Spectroscopy* 131.3 (2023).
- [13] Bekirov, Arlen R., et al. "Wave theory of virtual image." *Optical Materials Express* 11.11 (2021): 3646-3655.
- [14] Yan, Y., Li, L., Feng, C., Guo, W., Lee, S., & Hong, M. (2014). Microsphere-coupled scanning laser confocal nanoscope for sub-diffraction-limited imaging at 25 nm lateral resolution in the visible spectrum. *Acs Nano*, 8(2), 1809-1816.

[15] Allen, Kenneth W., et al. "Super-resolution microscopy by movable thin-films with embedded microspheres: resolution analysis." *Annalen der Physik* 527.7-8 (2015): 513-522.